Cognitive Stages in Learning Phases

Bachelor's Project Thesis

Isaiah van Hunen, i.van.hunen@student.rug.nl,
Supervisors: Hermine S. Berberyan & dr. Jelmer P. Borst

Abstract: This EEG study investigated which cognitive stages are present when solving a simple arithmetical task and what their qualitative changes with respect to learning are. We hypothesised there are cognitive stages that differ in occupation over three distinct learning phases, similar in characteristics to the cognitive, associative and autonomous phase as defined by Fitts and Posner (1967). To this end, we used an alpha-arithmetical task by Zbrodoff (1995) from which we obtained EEG-correlates. Using a bottom-up approach combining hidden semi-Markov modelling and multi-variate pattern analysis, we found that with practice the number of cognitive stages, response time and effect of task difficulty all reduced, substantiating multiple learning phases. However, the obtained cognitive stages remained dependent on task difficulty and did not fully conform to the characteristics of expected final learning phase.

1 Introduction

Learning is a process present in almost all organisms, both animal and plant, and even in artificial machines. The concept of learning encompasses a wide domain and although learning may occur after just one event, often it is a process of repeated events leading to knowledge and skill accumulation. Hence, practice makes perfect, but we don't yet know how. What then do we know about the mechanisms of learning? To answer this question, the current study shall apply the novel analysis technique of Hidden semi-Markov Model with Multi-Variate Pattern Analysis (HsMM-MVPA) on electroencephalography (EEG) correlates, to distinguish the cognitive stages present in solving an alpha-arithmetical task and examine their qualitative changes with learning.

Understanding the mechanisms of learning is important. If we can better understand these mechanisms that improve task performance, we can design tasks more effectively. In search of these mechanisms, we may start with considering the most visible effect of learning: the increase in one's performance in a simple task over time. Seeking to characterise this behaviour, the meta-analysis of Newell and Rosenbloom (1993) described the improvement in response time during practice, as a power function of the number of practice trials taken, dubbed "the Power Law of Practice". They ascribed this observed speedup to small qualitative changes in task execution, but do not discuss its cognitive nature. The Race Model, part of the Instance Theory of Automization (Compton and Logan, 1991; Logan, 1988) does propose underlying cognitive mechanisms of speedup. The Race Model states that each time a problem is solved, the answer is encoded in memory and when the problem is presented again, this encoded instance 'races' with similar instances for response generation. Furthermore, its predicted reduction of variability of response times over time fit well with experimental data.

However, one issue with either theory is they suggest a continuous speedup of a single learning phase, while the observed speedup may instead be attributed to qualitative changes between different learning phases. The Component Power Law Theory (CMPL) by Rickard (1997) states that there are two possible cognitive processes, calculation and the relatively faster retrieval of an answer. At any time, the current learning phase is determined by the dominant process used and, over time, the learning phase switches from the calculation to the retrieval phase, associated with a step-wise speedup in response time. Quantitative changes within these learning phases are possible too, building fluency in calculation and retrieval.

Offering another distinction of learning phases, Fitts and Posner (1967) suggest the cognitive, the associative, and the autonomous learning phase. These three phases were operationalised by Anderson in his Adaptive Control of Thought (ACT) theory and underlying learning mechanisms were identified in Adaptive Control of Thought-Rational (ACT-R) simulating skill acquisition (Anderson, 1990, 2007). ACT-R attributed two shifts in learning mechanisms to the three learning phases. The shift from the cognitive to the associative phase was marked by a shift from computation to retrieval. The shift from the associative to the autonomous phase was marked by a compilation of retrieval subprocesses into a reflexive production, relying on instant recognition of the problem and associated answer. Furthermore, ACT-R allows for speed-up within the first two learning phases through its mechanisms of knowledge compilation, collapsing multistep procedures into simpler and shorter procedures, and declarative strengthening, increasing the speed of retrieval. ACT-R has been well suited in modelling the interplay of cognitive processes and fitting behavioural data over a range of experimental studies.

Up to this point, most studies relied exclusively on behavioural data. To overcome the limitations of response time based methodology, the field of cognitive neuroscience has used neuroimaging to evaluate response time models. Borst and Anderson (2015) demonstrated the novel analysis technique of Hidden semi-Markov Model with Multi-Variate Pattern Analysis (HsMM-MVPA) that could distinguish qualitatively different temporal stages based on correlates of neuroimaging data. A HsMM-MVPA is a stochastic model that tries to identify a sequence of hidden states that underlie a set of given observations. In a HsMM, each state can correspond to several observations, making it so that the stages can be of variable duration (Yu, 2010). Their demonstration was further developed by Anderson, Zhang, Borst, and Walsh (2016), which was then used in a number of studies that successfully as a basis to discover and examine the underlying cognitive stages. In turn, this was used to test the pure insertion assumption (Zhang, Walsh, and Anderson, 2018b), examine cognitive mechanisms of association (Zhang, Walsh, and Anderson, 2017) or even map working memory both spatially and temporally (Zhang, van Vugt, Borst, and Anderson, 2018a). HsMM-MVPA seems promising and suitable for a wide range of neuroscientific research. How may we then apply this powerful method to investigate the progress of learning?

In order to investigate effects of practice, Tenison and Anderson (2016) used response time data of a practice task for HMM analysis (similar to HsMM), to find three distinct learning phases. Each phase showed speedup with practice, however, most speedup was produced by the transitions between the learning phases. Furthermore, they find parallels to the phases of skill acquisition proposed by the ACT-R theory; the cognitive, associative, and autonomous learning phase. In order to investigate the underlying cognitive stages in a single task and their changes with learning phase, they continued their research using functional magnetic resonance imaging (fMRI) data for HsMM-MVPA and find three cognitive stages: Encoding, Solving, and Responding (Tenison, Fincham, and Anderson, 2016). These stages show similar patterns to the mechanisms used in ACT-R simulations, where the first learning phase is dominated by a Solving stage while the last learning phase is dominated by the Responding stage. However, we assume there are more temporally distinct cognitive stages than this study could capture due to the low temporal resolution of fMRI. Therefore, the current study shall apply HsMM-MVPA on electroencephalography (EEG) correlates instead, to distinguish temporally close cognitive stages.

Previous studies have used a variety of tasks to study the effects of practice, each with their own advantages and disadvantages. Lebiere (1999) described a model of an alpha-arithmetical task (Zbrodoff, 1995) and observed a speedup due to learning phase transitions. This task consisted of problems such as 'A+2=C' where participant had to count on the left-hand side using the alphabet and then confirm or reject the equation. This task was also later implemented in the ACT-R tutorial (Bothell, 2009) which indicated there to be three learning phases. Furthermore, adults approach the problem similar to how children learn arithmetic and do not direct rely on retrieved numerical knowledge, due to the task's partially alphabetical nature (Barrouillet and Fayol, 1998). For these reasons, the Zbrodoff task is a suitable task to study the learning phases of practice on.

In the current study, we investigated which cognitive stages are present in solving a simple arithmetical task and what their qualitative changes are with respect to learning. We observed the effects of learning in the context of a Zbrodoff task, suitable due to its arithmetical yet novel nature. We then used HsMM-MVPA on EEG-correlates to obtain cognitive stages of fine temporal resolution. We hypothesised there are some defined cognitive stages that differ in occupation over three distinct learning phases, similar in characteristics to the cognitive, associative and autonomous phase.

2 Method

2.1 Participants

29 university students between the ages 18 and 32 participated in this study. All were right-handed, had normal or corrected-to-normal vision and no neurological disorders. All participants provided written informed consent and were monetarily compensated. Six participants were excluded for analysis; one participant due to having a non-Latin alphabet in their native language, three participants due to incomplete EEG data, one participant because of excessive ocular movements in EEG data and one participant because of inconsistencies between behavioural and EEG data. The analysis was performed on the data of the remaining 23 participants (12 females; $M = 23.6$ years, $\sigma = 3.93$). The study was performed according to the rules of conduct imposed by the Ethics Committee (CETO) of the Faculty of Arts of the University of Groningen, including the voluntary character and the absence of individual identifiers.

2.2 Task design

The participants were asked to identify novel mathematical equations as correct on incorrect using a simple keyboard response, based on Zbrodoff (1995). The mathematical equations used were in the format of 'A+2=C', where alphabetical characters referred to their index in the alphabet. As such, this equation would be correct as indeed 'C' occurs two places later than 'A' in the alphabet. An example of an incorrect equation would be 'A+3=B' as B does not occur three places later than 'A' in the alphabet.

The experiment used the addends '+2', '+3' and '+4', reflecting various difficulties. On the left hand side of the equations, 6 different 'left-side' characters (A to F) were used. On the right hand side of the equations, 8 different 'right-side' characters (C to K) were used as corresponding possible answers. Each of 3 addends was combined with 2 left-side characters, which were then finally combined with 2 right-side characters, one completing the equation to form a correct equation and one forming an incorrect equation. This resulted in 12 unique equations that were presented throughout the experiment, of which exactly half were correct. Each of these unique equations were presented 16 times per block and 48 times throughout the entire experiment. There was a total of 192 trials per block and 576 trials in total.

2.3 Procedure

Firstly, participants received the instruction to identify the mathematical equations as correct or incorrect with a keyboard response using only their right hand. Furthermore, they were instructed to refrain from using their fingers to count. They then completed one practice round of 6 trials that used different characters than in the rest of the experiment, followed by three blocks of 192 trails with two breaks per block.

A trial started with a black fixation dot in the centre of a white background presented for a random, variable duration between 500 and 1500 ms. Then, the stimulus was presented as a simple, 5-character equation separated with spaces (e.g. 'A + 2 = C') in black in the centre of a white screen, using the font 'Droid Sans Mono', size 20px. An answer could be given during the following 10 000 ms using the keys 'b' and 'n' for identifying the equation as correct or incorrect, respectively. After either the response or 10 000 ms, feedback would be presented for 1000 ms in the same black font in the middle of the screen ('Correct!', 'Incorrect' or 'Late'). This trial format is visually represented in Figure 2.1. Halfway and at the end of each block, the participant was given a break and shown the average response time and accuracy of that block.

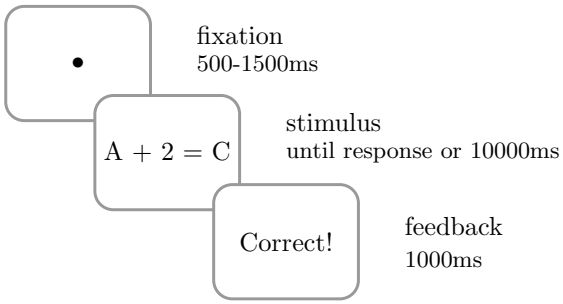

Figure 2.1: Example trial set-up

2.4 Behavioural analysis

Two behavioural measures were collected, accuracy and response time. Firstly, per condition of addend and block and per participant, trials with a response time outside 3 standard deviations of the mean were discarded, 1.8 % of all trials. Subsequently, to evaluate differences in accuracy in the various conditions, a linear mixed-effects model (LME) was fitted on the accuracy of trials, with the condition as fixed effect and the participant as a random effect. The LmerTest R package was used to obtain p-values for fixed effects based on Satterthwaite's method (Kuznetsova, Brockhoff, and Christensen, 2017). Then, trials with incorrect responses were discarded and another LME model was fitted on the participants' response times with the same fixed and random effects.

2.5 EEG recording and preprocessing

The EEG was recorded from 32 electrodes using active Ag-AgCI electrodes (Biosemi Active Two system). The recording had a sampling rate of 512 Hz and all scalp impedances were kept below 30 Ω. These electrodes were positioned according to the 10-20 layout system and two reference electrodes were placed on the mastoids. Data were then post-hoc referenced to the average of the mastoid electrodes. Furthermore, 4 electrodes were placed surrounding the left eye to record eye movements.

For preprocessing and analysis, the EEG data were then preprocessed using the EEGLAB toolbox (Delorme and Makeig, 2004) and custom scripts running on MATLAB (MATLAB, 2020). Firstly, the data were subjected to a low-pass filter of 1 Hz and a high-pass filter of 40 Hz and downsampled to 256 Hz. Artefacts were rejected manually, leading to a reduction of 1.85 % of data on average. Subsequently independent component analysis (ICA) was performed with EEGLab's *runica* function, using a logistic infomax algorithm (Bell and Sejnowski, 1995). On average, 1 to 2 components were then subtracted to remove eye blinks or muscle activity. Removed channels were topographically reconstructed using spherical spline interpolation.

2.6 HsMM-MVPA preprocessing

For the processing of the data for HsMM-MVPA, the data were first downsampled further to 100Hz to allow for faster computations. The data were then epoched on a trial-by-trial basis from stimulus onset to consecutive response. Outliers were removed according to the same criteria as for behavioural analysis (see Section 2.4). Also, trials with a duration of less than 500ms were rejected (constituting less than 0.5% of the data), allowing the determination of a sufficient number of cognitive stages in the subsequent analysis. The HsMM-MVPA would use all the data points between the stimulus and the response of all trials. A 400ms baseline was computed and subtracted from each epoch and any incomplete trials, induced by artefact rejection, were removed. A covariance matrix was computed for each trial and subject separately (Portoles, Borst, and van Vugt, 2018). Secondly, to reduce the dimensionality of the highly intercorrelated EEG sensory data, a principal component analysis (PCA) was performed in preparation for HsMM-MVPA. The first 10 components accounted for 94.8% of the variance of the EEG signal. Lastly, the data were normalised using z-scores. This transformed data are the EEG-correlates used for the subsequent analysis.

2.7 HsMM-MVPA

In our case, the HsMM-MVPA will identify the cognitive stages given the observations of all EEG data from stimulus to response per trial. The HsMM-MVPA method used is based on the study of Anderson et al. (2016). The HsMM-MVPA identifies brief sinusoidal peaks as its states, termed 'bumps'. The regions between bumps are termed 'flats', periods with a mean amplitude of zero reflecting a

distinct cognitive stage. A number of assumptions are made to facilitate analysis. Firstly, bumps are assumed to follow the shape of a half-sine and last 50ms. Because all trials minimally last 500ms, this means maximally 10 bumps can be fit. Secondly, the HsMM-MVPA model assumes these bumps do not overlap. Thirdly, the flat durations are assumed to follow a gamma distribution with a shape parameter of 2. An n-bump model estimates $n+1$ cognitive stages between the stimulus presentation and the response, separated by those bumps. The model assesses the log-likelihood of a particular bump placement as well as its associated flat gamma duration, per individual trial. The model then maximises the summed log-likelihood of these across all trials using a standard Expectation-Maximisation (E-M) algorithm. This involves the computationally expensive process of considering all possible placements of the bump locations, which the dynamic programming of HsMM-MVPA is very suitable for.

The fitting process of bumps and flats requires initial bump amplitudes and gamma distributions which will be used for the E-M algorithm. The outcome of this algorithm is very sensitive to the initial starting points however. To avoid ending up in local maxima, our approach is based on that of Zhang et al. (2018b). The initial parameters are obtained from fitting a separate model per condition on the maximum number of bumps $n_{\max} = 10$. Then, to construct models with $n_{\max-1}$ bumps placed at various locations, these parameters are used a starting point. Of these models, only the model with the best fit (highest log-likelihood) is retained and its parameters are used as starting point for the generation of the next $n-1$-bump models. This process continues down to the 1-bump model. By starting with the maximum number of bumps, this approach aims to preserve the bump topologies and avoid local maxima.

The HsMM-MVPA generates models of cognitive stages increasing in number of bumps and therefore also increasing in degrees of freedom and thus in log-likelihood. To avoid overfitting, a leave-one-out cross-validation (LOOCV) procedure was applied, comparing models based on their both log-likelihood and their parsimony. Per HsMM-MVPA model, the model was created based on the data of all but one participant and then subsequently fitted on that remaining participant, obtaining a log-likelihood. This was repeated for all participants. The overall log-likelihood of the model was taken as the mean of all LOOCV log-likelihoods. Secondly, the significance of the difference in log-likelihood for n-bump and $n+1$-bump models was investigated. For each such pair, a comparison was made for how many subjects the log-likelihood increased with the more complex $n+1$-bump models. Then, a sign test was used on this ratio p to determine if a significant number of participants improved from $n-1$ to n bumps. This enabled the verification of whether a model sufficiently outperformed a more parsimonious model, warranting its increased complexity.

2.8 HsMM-MVPA model selection

To allow experimental conditions to shape the HsMM-MVPA model, the model can be made separately on the data of different conditions. As such, one model was made on all available data, one model was made per block condition, another model was made per addend condition and lastly one model was made per block per addend. Then, the fit of these models was compared to select the best overall fit to the data, while keeping in mind for different conditions, different amount of bumps may fit best. Lastly, for the selected model, bumps of the underlying sub-models per condition were mapped to one another, to investigate whether the model could be simplified by sharing cognitive stages across conditions.

3 Results

3.1 Behavioural results

Behavioural results were gathered in the form of response times and accuracy. Figure 3.1 shows the response time per addend per block. Firstly, we observe a decreasing effect of block on response time, the largest from block 1 to 2. This reflects exposure to the task facilitating learning, which in turn lowers response time. Secondly, we observe an increasing effect of addend on response time, but not between addend 3 and 4. Addend 2 has lower associated response times than both addends 3 and 4, reflecting reduced difficulty of the task lowering response time. Lastly, between block 1 and 2, the

decrease in response time is somewhat larger for addend 4 than for the other addends. That is, the initial reduction of response time is larger for the most difficult task condition. These conclusions are supported by the results of the LME models, showing significant effects for block, addend (excluding 3-4) and interactions (see Table 3.1).

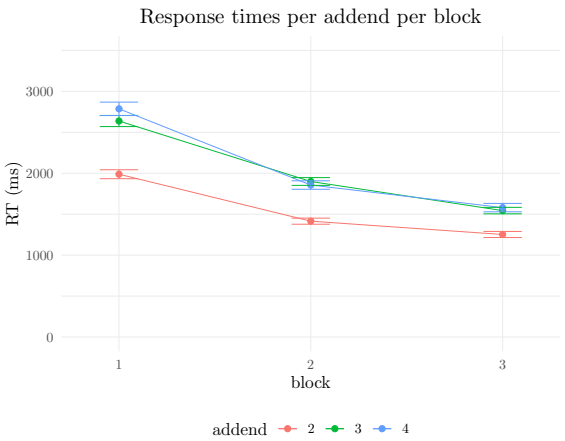

Figure 3.1: Response time per addend per block in milliseconds. Error bars denote the 95% CI of the within-subject standard error.

	Response time		
	Estimate	t value	p-value
Intercept	2,027.16	11.26	< 0.001 ***
Addend 3	669.36	18.19	< 0.001 ***
Addend 4	922.60	25.06	< 0.001 ***
Block 2	-591.92	-16.05	< 0.001 ***
Block 3	-757.39	-20.52	< 0.001 ***
Addend 3:Block 2	-182.67	-3.51	< 0.001 ***
Addend 4:Block 2	-463.35	-8.89	< 0.001 ***
Addend 3:Block 3	-372.03	-7.13	< 0.001 ***
Addend 4:Block 3	-569.70	-10.92	< 0.001 ***

Table 3.1: LME model of response time

Figure 3.2 shows the accuracy per addend per block. Firstly, we observe that from block 1 to 2 the accuracy increases, mostly so for addend 4. That is, the initial improvement in accuracy is primarily seen in the most difficult task condition. The accuracy does not seem to increase from block 2 to block 3, indicating an absence of further improvement in accuracy over time. The accuracy remains at around 95 % indicating good performance overall. Overall, the accuracy is lower for addend 4 compared to addends 2 and 3, which do not differ much from each other on all blocks.

These conclusions are supported by the results of the LME models, showing significant effects for block and addend (excluding 2-3) (see Table 3.2).

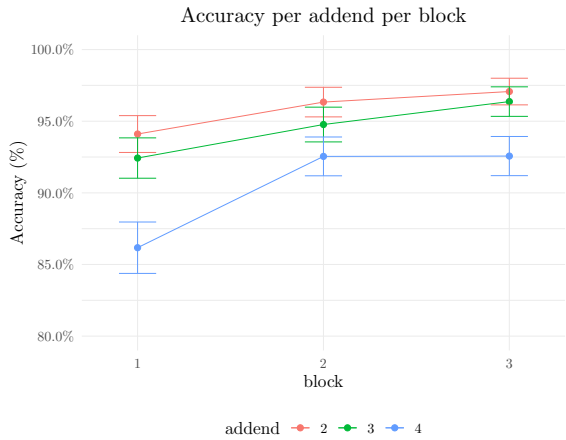

Figure 3.2: Accuracy per addend per block in percentages. Error bars denote the 95% CI of the within-subject standard error.

	Accuracy		
	Estimate	z value	p-value
Intercept	3.241	12.35	< 0.001 ***
Addend 3	-0.285	-1.86	0.06
Addend 4	-1.019	-7.30	< 0.001 ***
Block 2	0.520	2.86	< 0.01 **
Block 3	0.761	3.90	< 0.001 ***
Addend 3:Block 2	-0.103	-0.43	0.67
Addend 4:Block 2	0.232	1.04	0.30
Addend 3:Block 3	0.056	0.21	0.83
Addend 4:Block 3	-0.005	-0.02	0.98

Table 3.2: LME model of accuracy

3.2 ERP results

Both stimulus-locked and response-locked ERP waveforms were obtained over twelve scalp regions, combinations of frontal, central, parietal and occipital regions, left, centre or right*, aggregated per

*Corresponding to EEG channels F3 Fz F4, C3 Cz C4, P3 Pz P4, O1 Oz O2 from left to right, top to bottom respectively.

block or per addend. Subsequently, the differences between each set of three conditions were pairwise evaluated using the t-test and the Benjamini-Hochberg procedure to control the False Discovery Rate (FDR; Benjamini and Hochberg, 1995). The response-locked ERPs per block are presented in Figure 3.3 and other combinations in Appendix A.

Firstly, we observe significant differences only between blocks, not between addend conditions. Secondly, more significant differences arise in response-locked than in stimulus-locked ERP waveforms. Thirdly, significant differences arise mostly between block 1 and 3, less so in between block 1 and 2 or 2 and 3.

Observing the response-locked ERPs per block in Figure 3.3, the learning process contributed additively to mean voltages over middle and right-lateralised frontal regions prior to response, and subtractively to mean voltages over left-lateralised posterior regions after response. Other significant effects of conditions are not observable. Because the differences in ERPs were mostly observed when comparing block 1 and block 3 and because the HsMM-MVPA is modelled on EEG-correlates, we decided to make HsMM-MVPA models for only these blocks.

3.3 HsMM-MVPA results

3.3.1 Model comparison

Various HsMM-MVPA models were made on the EEG-correlates of block 1 and 3, being either based on all data, per block, per addend or per block and addend. The resulting loglikelihoods per number of bumps are presented in Figure 3.4. We may first observe that across most bumps, the block and addend separated model has a higher mean loglikelihood than all other models. Secondly, all models have an overall maximal likelihood at 6 bumps. Although the block and addend separated separated model has the highest mean likelihood, upon further inspection it displayed few differences per addend and may be subject to over-fitting. We tentatively reject the maximally separated model for now and investigate the model of second highest loglikelihood, separated per block.

Next, we compared the likelihood of this model per bump across block 1 and block 3, presented in Figure 3.5. For block 1, the highest loglikelihood with a significant improvement, as compared to a simpler model with one less bump, is the bump-6 sub-model. This sub-model is favourable compared to the block 1 bump-7 sub-model which does not significantly outperform the simpler 6-bump model.

For block 3, there is no sub-model with a significant improvement compared to a simpler sub-model. Therefore, we will choose the bump-5 sub-model with the highest loglikelihood instead. We shall call the combined bump-6 block 1 and bump-5 block 3 the 'bump-selected block model' from now on, visually presented in Figure 3.4 at the average number of bumps, 5.5. Before selecting this model as the best model, the summed likelihood of this model was compared to that of previously considered bump-6 block and addend separated model. To this end, the models were compared, both using 5 bumps for block 1 and 6 bumps for block 3. This maximally separated model did not outperform the simpler bump-selected block model as it improved in loglikelihood for only 16 of 23 participants, not significant according to a sign test (also indicated in the Figure 3.4 with "n.s."). Therefore, we will favour the bump-selected block model due to its reduced complexity and use it for further evaluation.

3.3.2 Model inspection

The bump-selected block model has 6 bumps in block 1 and 5 bumps in block 3, with position and topologies as displayed in Figures 3.6 and 3.7. We may observe that for both blocks, the initial four bumps share similar topology patterns and onsets across blocks, although differing in scale. A possible simplification of the model can be made by having block 1 and 3 sub-models share bumps. To this end, combinations of the first four bumps were mapped by taking their mean parameters and the resulting likelihood was as presented in Figure 3.8. We observe some bump combinations map better than others. Most notably, the most simple model that shares the initial four bumps is not outperformed by the non-mapped model, nor by any other more complex mapping combination (not shown). Therefore, we will select this model as our final model, as it is the least complex model not outperformed by more complex models.

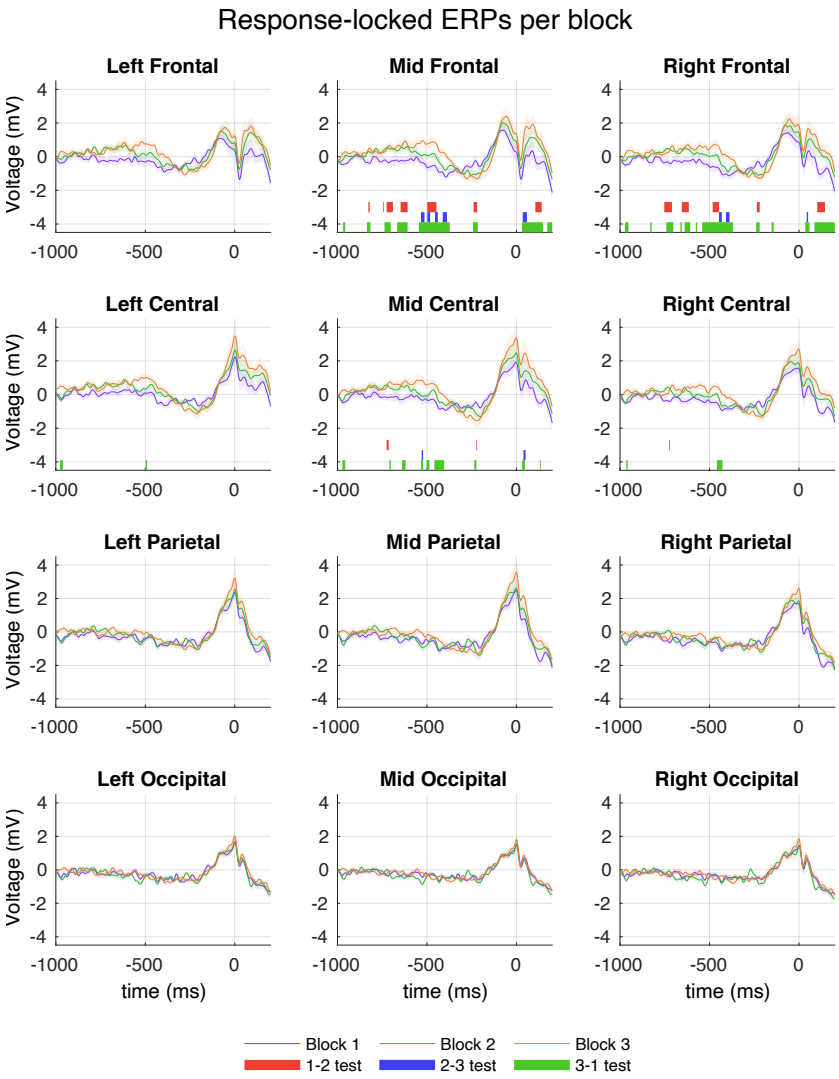

Figure 3.3: Response-locked ERP waveforms from twelve regions for three block conditions. Shaded areas indicate standard error of ERP signal of block associated by color. Bars at the bottom of the graphs indicate temporal regions of Benjamini-Hochberg corrected significance, pairwise as block 1-2, 2-3 and 3-1. Addend conditions and stimulus-locked waveform comparisons are included in Appendix A.

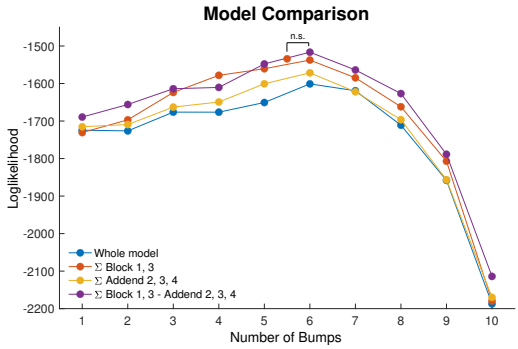

Figure 3.4: Comparison of likelihood of HsMM-MVPA models varying in condition separation. The point at 5.5 bumps indicates the loglikelihood of the bump-selected model. "n.s." indicates the non-significant improvement of the block and addend separated model (at bump-6 block 1 and bump-5 block 3) over the bump-selected block model.

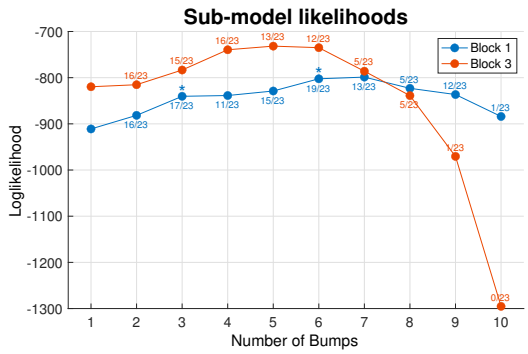

Figure 3.5: Likelihoods of HsMM-MVPA sub-models of block 1 and block 3 respectively. Ratios indicate the proportion of subjects p for which there is an improvement over the $n-1$-bump of the same sub-model. Asterisks indicate significant improvement where $p \geq 17$.

3.3.3 Cognitive stage interpretation

As we have now obtained a final model, a functional interpretation of its bumps, based on their topologies and onsets, can be made. Our first stages showed a striking similarity to Berberyan, van Maanen, van Rijn, and Borst (2020) (submitted). We therefore closely follow her interpretation, with additions from the studies by Zhang et al. (2017; 2018a).

As the first bump in those studies, the current first bump also has a central-parietal negativity and early onset of 100 ms. This is characteristic of an N1 ERP component, typically interpreted as an index of visual attention (Luck, 2005). As such, the cognitive stage 1 is most likely a 'Pre-attention stage'. The second bump has a prominent frontal positivity and an onset of 200 ms. This is characteristic of an P2 ERP component, associated with attention (Miltner, Johnson, Braun, and Larbig, 1989; Rugg, Milner, Lines, and Phalp, 1987) making cognitive stage 2 most likely an 'Attention' stage, handling the initial interpretation of the presentation format. The third bump displays a central-frontal positivity and onset of 400 ms. The topology matches that of a P3a ERP component associated with engagement of attention and processing of novelty (Polich, 2003). The onset is quite late for a P3a ERP component however, this bump may instead be the dissipation of activation of bump 2. We shall label cognitive stage 3 a 'Attention orienting' stage. The fourth bump differs in scale between block 1 and 3 and displays a posterior-anterior gradient of increasing, lateralised positivity for both blocks. This, together with its onset of 400 ms, is similar to the FN400 ERP component, widely accepted as an index of familiarity-driven recognition (Curran, 2000; Mark and Rugg, 1998). Thus, this stage may be involved in participants' judgement of whether this problem was familiar, and thus whether it was worth attempting a retrieval process. This leads to our interpretation of cognitive stage 4 as a 'Recognition' stage. Until the fourth bump, our stages are conform Berberyan et al., however, the following bumps and their interpretations are specific to our experiment.

The fifth bump is different across block 1 and 3. First, let us consider block 1. The fifth bump displays a large frontal negativity, not directly matching well-known ERP components. Further-

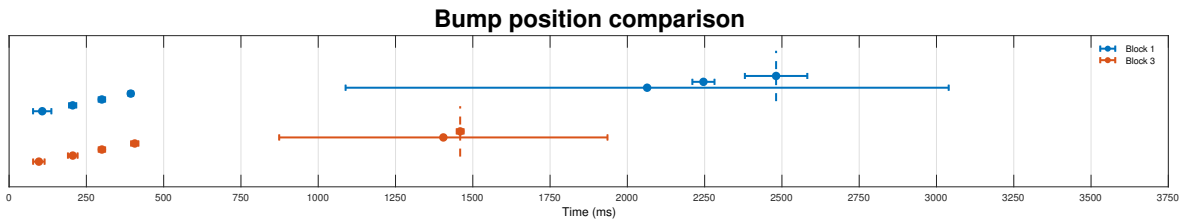

Figure 3.6: Position of the bumps of the bump-selected block model relative to stimulus onset. The vertical dashed line indicates the time of response.

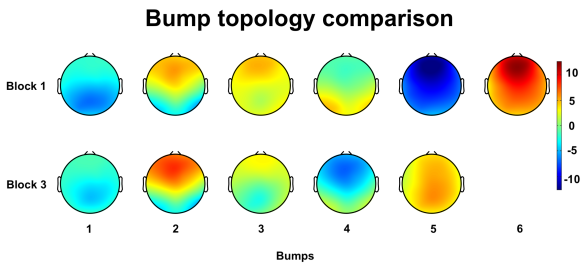

Figure 3.7: Topologies of the bumps of the bump-selected block model.

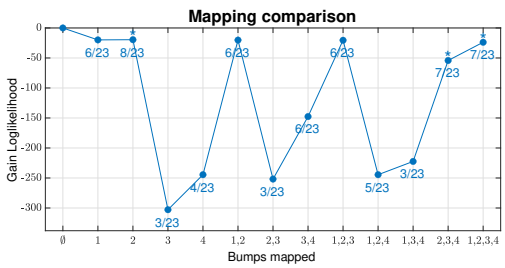

Figure 3.8: Comparison of likelihood of various mappings of bumps of block 1 and block 3 model. Above each point is indicated the ratio of subjects p for which the likelihood improved as compared to no mapping. Asterisks indicate a non-significant improvement of non-mapped model to the mapped model where $23 - p < 17$.

more, this bump has an onset of more than 1000 ms later than the previous bump and is dependent in onset (and thus prior stage duration) on the addend. This process lasts longer for higher addends, similar to the Solving process of the study of Tenison et al. (2016). Most likely, this stage is involved in the advancement of characters along the alphabet, including any retrieval of the alphabet's order, as these processes would last longer for higher addends, as well as matching the calculated answer to the presented right-hand side called response mapping. Therefore, we label cognitive stage 4 of block 1 the 'Calculation and Response mapping' stage. Regarding cognitive stage 5, this stage may have been involved in storing the correct answer in memory for later reuse, providing a basis for participants' speedup over time. This would then make cognitive stage 5 of block 1 a 'Memory storage' stage. The sixth bump of block 1 displays a strong frontal positivity and occurs about 250 ms prior to the response. As the sixth cognitive stage is followed by response execution, it is most likely involved in the necessary motor planning, making cognitive stage 6 the 'Response' stage.

Regarding block 3, as it has one less bump than block 1, it may be that the fifth bump of block 3 includes both processes in bumps 5 and 6 of block 1. As bump 5 of block 3 shares its duration dependency on addend with bump 5 of block 1 but to a lesser degree, it may be partially involved in calculation too. Furthermore, bump 5 of block 3 shares its frontal positivity with bump 6 of block 1, suggesting involvement in memory processes, most likely memory retrieval. Also it is likely that this process matches the generated answer to the correct response. Therefore, the cognitive stage 4 of block 3 may be labelled the 'Retrieval, Calculation and Response mapping' stage, followed by a 'Re-

sponse stage' as in block 1. These stages and previous conclusions are visually presented in Figure 3.9.

4 Discussion

The aim of this study was to investigate which cognitive stages are present in solving a simple arithmetical task and what their qualitative changes are with respect to learning. This study used an alpha-arithmetical task to observe the effects of practice. Furthermore, it used HsMM-MVPA on EEG-correlates to obtain cognitive phases. Following studies that inspected learning phases of similar arithmetical tasks, we hypothesised there are defined cognitive stages that differ in occupation over three distinct learning phases, similar in characteristics to the cognitive, associative and autonomous phase.

Firstly, the behavioural analysis shows clear evidence of learning over the course of the experiment, reducing response times and increasing accuracy for all blocks. Furthermore, per block the effect of addend decreases, suggesting a decrease of dependency on addends for cognitive phases as learning phases transition, akin to study of Tenison et al. (2016). However, in the last block response times remain distinctly shorter for an addend of 2, compared to the other addends, which is contradictory to our hypothesis; although there is evidence of different learning phases, the last learning phase reached does not fully conform to characteristics of the associative or autonomous phase of Tenison and Anderson (2016).

One possible cause of this remaining addend dependency of the last learning phase lies in the presentation format. Throughout the experiment, the full equation was presented as 'A+2=D' where participants had to judge its validity. It is likely that upon answering, participants memorised this full equation along with its binary answer, instead of merely the left-hand side of the equation alongside its (calculated) alphabetical answer. This is in contrast to the study of Tenison et al., where participants had to calculate a numerical answer and associate this with the problem presented. This presentation format may have led to increased interference in retrieval with similar encoded answers. That is, this format has a high degree of similarity between presented visual items, sometimes their entire left hand side, and a high degree of similarity between encoded binary answers. As such, a stored presentation of 'A+2=C' as 'valid' may have interfered with the retrieval process of the correct answer to a presentation of 'A+2=D', given their overlap of the left hand side. This may have prevented participants from successfully and distinctly encoding and retrieving answers and so reaching the associative phase and fully removing addend dependency. To avoid this complication, the study could be adapted to present only the left side of the equations itself and ask the participant to complete i.e. 'A+2=?'. This alternative format would prompt participants to initially calculate the alphabetical answer and largely prevent associations across different presentations. This adaptation would result in a larger set of keys corresponding to a possible answer, influencing response execution. To prevent subsequent variability in duration and cognitive processes, the experiment should therefore ask participants to first press e.g. the spacebar and only then indicate the correct answer using an alphabetical key in a limited timeframe. Including this possible interference, the final model of this study does show a speedup, reduction of cognitive stages and decrease of effect between addends 3 and 4 across blocks, supporting our hypothesis to a large degree.

Furthermore, the improvement in both response time and accuracy is visibly largest between block 1 and 2. It could well be that the two transition between three learning phases have a different effect on behavioural measures, that is that the first transition produces the largest speedup. Alternatively, it could be there are only two learning phases, block 1 and block 2 & 3. However, this latter interpretation is incongruent with the ERP waveforms as cognitive index, which display mostly significant differences between block 1 and 3, rather than between block 1 and 2 (or block 2 and 3). It may well be there is a mixture of three learning phases, not well-separated over the experimental blocks. In order to interpret these phases distinctly, a division of learning phases could be made on the basis of the latency data using HsMM, as in the study of Tenison and Anderson. A pitfall of such an approach would be the increased risk of overfitting introduced by applying both HsMM-MVPA to latency data to determine learning phases and to neural correlates to determine cognitive stages, although exciting.

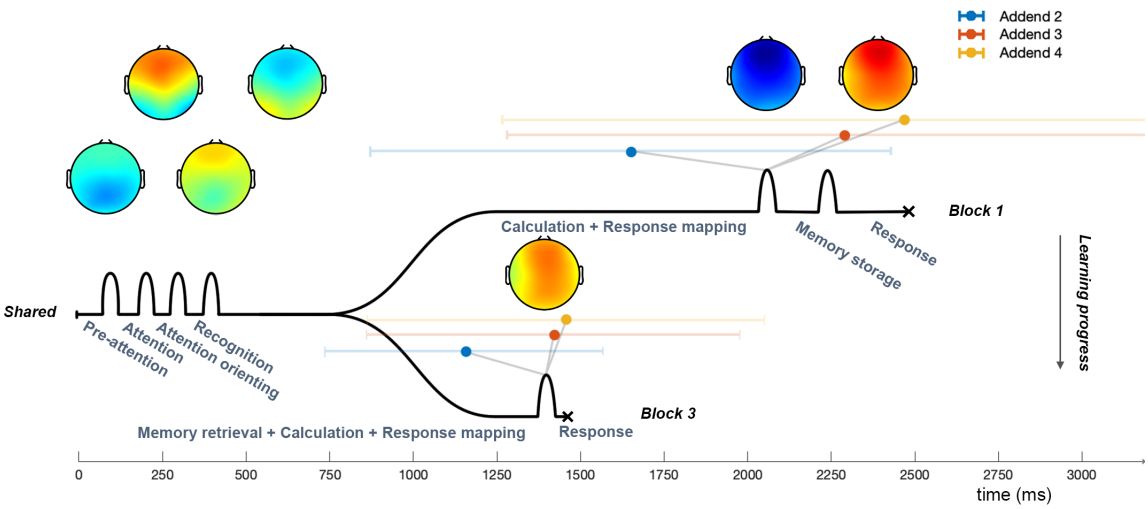

Figure 3.9: Bump topologies, onsets and stage interpretation of final model. Time is relative to stimulus onset and cross symbols indicate response execution. For the fifth bumps, the underlying onset per addend and standard deviations thereof are displayed.

Moreover, the effect of addend appears non-linear too. The response times differ mostly between addend 2 and addends 3 and 4. It may be that for the lower addends a different strategy was used than for higher addends, resulting in faster response times. However, the EEG waveforms show no evidence of different cognitive processes for different strategies. Further complicating the matter, the accuracy shows an another separation, where accuracy differs mostly between addends 2 and 3 and addend 4. Thus, for two different strategies, it is unclear for which addends they would have been used. To evaluate the possibility of strategies per addend, the addends used could be extended to also include 5 and 6, and then inspect if a clear division of behavioural measures between addend ranges becomes apparent. One possible effect of addend unaccounted for, is that only the start of the alphabet was used as base, A to F, such that the lower addend of 2 extends less far in the alphabet. It is likely characters this early in the alphabet are more accessible to retrieval than later characters, as these are more used in everyday alphabetical numbering, mathematics, etc. This makes an addend of 2 disproportionally likely to remember, compared to addends 3 and 4. This also further complicates determining the moment of learning phase transitions as discussed before; it may be that for lower addends the transition in learning phase to the associative and autonomous phase occurs earlier than for higher addends. This effect may be avoided by simply using a character range placed later in the alphabet such as J to O, where the beginning of the total range of characters used in the experiment, is not more familiar to participants than the end.

Regarding the cognitive stages, we found evidence of 6 and 5 distinct cognitive stages respectively at the beginning and the end of the practice task. The initial four stages are shared across blocks while the last stages are specific per block. These initial four stages pertain to visual recognition processes largely independent of the task. This is also found in previous literature on simple visual tasks with HsMM-MVPA on EEG-correlates, demonstrating the reliability of HsMM-MVPA in finding these stages. Furthermore, we found more cognitive stages in the first block than in the last, supporting distinct learning phases. The reduction of cognitive stages over blocks mirrors the mechanisms of ACT-R's learning phase transitions; knowledge compilation and the collapse of multi-step procedures. On the other side, the last block still displays a longer stage dependent on addend, and therefore likely involved in calculation (called the Solving stage in Tenison and Anderson). It must be noted this observation is the same as the

remaining dependency of response time on addend as previously discussed.

Furthermore, the amount of learning phases cannot be verified on the basis of the HsMM-MVPA results, as only two blocks were used. However, if the moment of transition of learning phases could be well determined beforehand (possibly with HsMM-MVPA on latency data as discussed before), the cognitive stages found per learning phase could be used to investigate their qualitative differences in terms of their number and topology per learning phase.

With regard to the model selection of HsMM-MVPA, it must be noted the selection made is not without its challenges. Sign tests were used to balance parsimony and fit of a model, but this could not avoid a difficult selection procedure. This study faced four possibilities of model separation; all data (A), per block (B), per addend (C) or per block and addend (D), respectively increasing in complexity and loglikelihood. The best fitting model D outperformed the simplest model A based on a significant sign test and was thus interpreted as preferable. The second best fitting model B was not outperformed by the most complex model D, and was also its subset (discarding differences per addend), and thus preferred above model D. However, this model B did not significantly outperform the simplest model A itself, based on a sign test. This in turn implies that model A should be preferred above model B. This apparent cyclic reasoning is the result of the thresholding that is the core of frequentist statistics, together with a continuous accumulation of loglikelihood over increasing levels of complexity. There exists no undisputed decision to this conflict. This study has selected model B as the best fit, based on ERP data which displayed significant differences in block and none for addends. It may be that there exist interactions of addend and block, that is, possibly for some addends, there exist distinctly different cognitive phases per block than for other addends. This could be possible if indeed different strategies were used per addend, affecting the rate and processes of learning, as discussed earlier. Introducing more addend conditions would therefore also shed light on such possible interactions and in turn, aid HsMM-MVPA model selection. However, adapting model selection to possible addend interactions would require a more rigorous selection procedure than the currently used method, as the number of possible models would vastly increase and most likely contain more cyclic and contradictory model preferences.

Lastly, per definition cognitive 'stages' describe the parts of a serial process. However, it is likely that a practice task does not consist of only serial processes, but contains parallel, partially overlapping processes as well. HsMM-MVPA provides topology, onset and duration of cognitive stages, but it is not suited to model parallel cognitive processes. As such, we attributed multiple functions to a single cognitive stage to explain the observed characteristics, such as both memory retrieval, calculation and response mapping. Although it is likely these are all present to various degrees, one should be careful with multiple functional interpretations based on a single bump's characteristics. Therefore, we see an opportunity for further research to investigate the extent to which functional interpretation of cognitive stages based on HsMM-MVPA holds and explore possible approaches of dealing with the partially parallel nature of cognitive processes.

The findings of this study on the progress of practice are largely specific for the task used. The HsMM-MVPA method used shows great promise in unraveling underlying cognitive stages and informing us on qualitative cognitive differences between conditions. This study is part of the development of the neuroscientific field, replacing pure behavioural characterisations with an analysis of the mixture of underlying cognitive stages instead. However, dependent on the spatial and temporal resolution of the data used, functional interpretation of these cognitive stages remains difficult. We look forward to more applications of HsMM-MVPA on neuroimaging data able to combine both a high temporal and spatial resolution, possibly through combining EEG and fMRI techniques.

5 Acknowledgements

This research used data as collected in Shouche (2019), for which the author is thankful. Furthermore, the author would like to sincerely thank Hermine Berberyan and Jelmer Borst for their supervision on this thesis.

References

John R. Anderson. *The Adaptive Character of Thought*. The Adaptive Character of Thought. Lawrence Erlbaum Associates, Inc, Hillsdale, NJ, US, 1990. ISBN 978-0-8058-0419-5.

John R. Anderson. *How Can the Human Mind Occur in the Physical Universe?* How Can the Human Mind Occur in the Physical Universe? Oxford University Press, New York, NY, US, 2007. ISBN 978-0-19-532425-9. doi: 10.1093/acprof:oso/9780195324259.001.0001.

John R. Anderson, Qiong Zhang, Jelmer P. Borst, and Matthew M. Walsh. The Discovery of Processing Stages: Extension of Sternberg's Method. *Psychological review*, 123(5):481–509, October 2016. ISSN 0033-295X. doi: 10.1037/rev0000030.

Pierre Barrouillet and Michel Fayol. From algorithmic computing to direct retrieval: Evidence from number and alphabetic arithmetic in children and adults. *Memory & Cognition*, 26(2):355–368, March 1998. ISSN 1532-5946. doi: 10.3758/BF03201146.

A. J. Bell and T. J. Sejnowski. An information-maximization approach to blind separation and blind deconvolution. *Neural Computation*, 7(6):1129–1159, November 1995. ISSN 0899-7667. doi: 10.1162/neco.1995.7.6.1129.

Yoav Benjamini and Yosef Hochberg. Controlling the False Discovery Rate: A Practical and Powerful Approach to Multiple Testing. *Journal of the Royal Statistical Society. Series B (Methodological)*, 57(1):289–300, 1995. ISSN 0035-9246.

Hermine S. Berberyan, Leendert van Maanen, Hedderik van Rijn, and Jelmer P. Borst. EEG-based identification of evidence accumulation stages in decision making. 2020.

Jelmer P. Borst and John R. Anderson. The discovery of processing stages: Analyzing EEG data with hidden semi-Markov models. *NeuroImage*, 108:60–73, March 2015. ISSN 1053-8119. doi: 10.1016/j.neuroimage.2014.12.029.

Dan Bothell. ACT-R Tutorial distributed with ACT-R 6.0 version 1.3 r766., 2009.

Brian J. Compton and Gordon D. Logan. The transition from algorithm to retrieval in memory-based theories of automaticity. *Memory & Cognition*, 19(2):151–158, March 1991. ISSN 1532-5946. doi: 10.3758/BF03197111.

Tim Curran. Brain potentials of recollection and familiarity. *Memory & Cognition*, 28(6):923–938, November 2000. ISSN 1532-5946. doi: 10.3758/BF03209340.

Arnaud Delorme and Scott Makeig. EEGLAB: An open source toolbox for analysis of single-trial EEG dynamics including independent component analysis. *Journal of Neuroscience Methods*, 134(1):9–21, March 2004. ISSN 0165-0270. doi: 10.1016/j.jneumeth.2003.10.009.

P.M. Fitts and M.I. Posner. *Human Performance*. Human Performance. Brooks/Cole, Oxford, England, 1967.

Alexandra Kuznetsova, Per B. Brockhoff, and Rune H. B. Christensen. lmerTest Package: Tests in Linear Mixed Effects Models. *Journal of Statistical Software*, 82(1):1–26, December 2017. ISSN 1548-7660. doi: 10.18637/jss.v082.i13.

Christian Lebiere. The dynamics of cognition: An ACT-R model of cognitive arithmetic. *Kognitionswissenschaft*, 8(1):5–19, March 1999. ISSN 1432-1483. doi: 10.1007/BF03354932.

Gordon D. Logan. Toward an instance theory of automatization. *Psychological Review*, 95(4):492–527, 1988. ISSN 1939-1471(Electronic),0033-295X(Print). doi: 10.1037/0033-295X.95.4.492.

Steven Luck. *An Introduction to The Event-Related Potential Technique*. January 2005.

Ruth Mark and Michael Rugg. Age effects on brain activity associated with episodic memory retrieval. An electrophysiological study. *Brain : a journal of neurology*, 121 (Pt 5):861–73, June 1998. doi: 10.1093/brain/121.5.861.

MATLAB. Version 9.8.0 (R2020a). The MathWorks Inc., 2020.

Wolfgang Miltner, Ray Johnson, Christoph Braun, and Wolfgang Larbig. Somatosensory event-related potentials to painful and non-painful

stimuli: Effects of attention. *Pain*, 38(3):303–312, September 1989. ISSN 0304-3959. doi: 10.1016/0304-3959(89)90217-0.

A. Newell and Paul Rosenbloom. Mechanisms of skill acquisition and the law of practice. *Cognitive Skills and Their Acquisition*, Vol. 1, August 1993.

John Polich. Theoretical Overview of P3a and P3b. In John Polich, editor, *Detection of Change: Event-Related Potential and fMRI Findings*, pages 83–98. Springer US, Boston, MA, 2003. ISBN 978-1-4615-0294-4. doi: 10.1007/978-1-4615-0294-4_5.

Oscar Portoles, Jelmer P. Borst, and Marieke K. van Vugt. Characterizing synchrony patterns across cognitive task stages of associative recognition memory. *European Journal of Neuroscience*, 48(8):2759–2769, 2018. ISSN 1460-9568. doi: 10.1111/ejn.13817.

Timothy C. Rickard. Bending the power law: A CMPL theory of strategy shifts and the automatization of cognitive skills. *Journal of Experimental Psychology: General*, 126(3):288–311, 1997. ISSN 1939-2222(Electronic),0096-3445(Print). doi: 10.1037/0096-3445.126.3.288.

M. D. Rugg, A. D. Milner, C. R. Lines, and R. Phalp. Modulation of visual event-related potentials by spatial and non-spatial visual selective attention. *Neuropsychologia*, 25(1, Part 1):85–96, January 1987. ISSN 0028-3932. doi: 10.1016/0028-3932(87)90045-5.

Prajakta Shouche. *EEG Correlates of Learning in the Alpha-Arithmetic Task*. Bachelor's Thesis, University of Groningen, Groningen, 2019.

Caitlin Tenison and John R. Anderson. Modeling the distinct phases of skill acquisition. *Journal of Experimental Psychology: Learning, Memory, and Cognition*, 42(5):749–767, 2016. ISSN 1939-1285(Electronic),0278-7393(Print). doi: 10.1037/xlm0000204.

Caitlin Tenison, Jon M. Fincham, and John R. Anderson. Phases of learning: How skill acquisition impacts cognitive processing. *Cognitive Psychology*, 87:1–28, June 2016. ISSN 1095-5623. doi: 10.1016/j.cogpsych.2016.03.001.

Shun-Zheng Yu. Hidden semi-Markov models. *Artificial Intelligence*, 174(2):215–243, February 2010. ISSN 0004-3702. doi: 10.1016/j.artint.2009.11.011.

N. Jane Zbrodoff. Why is 9+7 harder than 2+3? Strength and interference as explanations of the problem-size effect. *Memory & Cognition*, 23(6):689–700, November 1995. ISSN 1532-5946. doi: 10.3758/BF03200922.

Qiong Zhang, Matthew M. Walsh, and John R. Anderson. The Effects of Probe Similarity on Retrieval and Comparison Processes in Associative Recognition. *Journal of Cognitive Neuroscience*, 29(2):352–367, February 2017. ISSN 1530-8898. doi: 10.1162/jocn_a_01059.

Qiong Zhang, Marieke van Vugt, Jelmer P. Borst, and John R. Anderson. Mapping working memory retrieval in space and in time: A combined electroencephalography and electrocorticography approach. *NeuroImage*, 174:472–484, July 2018a. ISSN 1053-8119. doi: 10.1016/j.neuroimage.2018.03.039.

Qiong Zhang, Matthew M. Walsh, and John R. Anderson. The Impact of Inserting an Additional Mental Process. *Computational Brain & Behavior*, 1(1):22–35, March 2018b. ISSN 2522-087X. doi: 10.1007/s42113-018-0002-8.

A Appendix

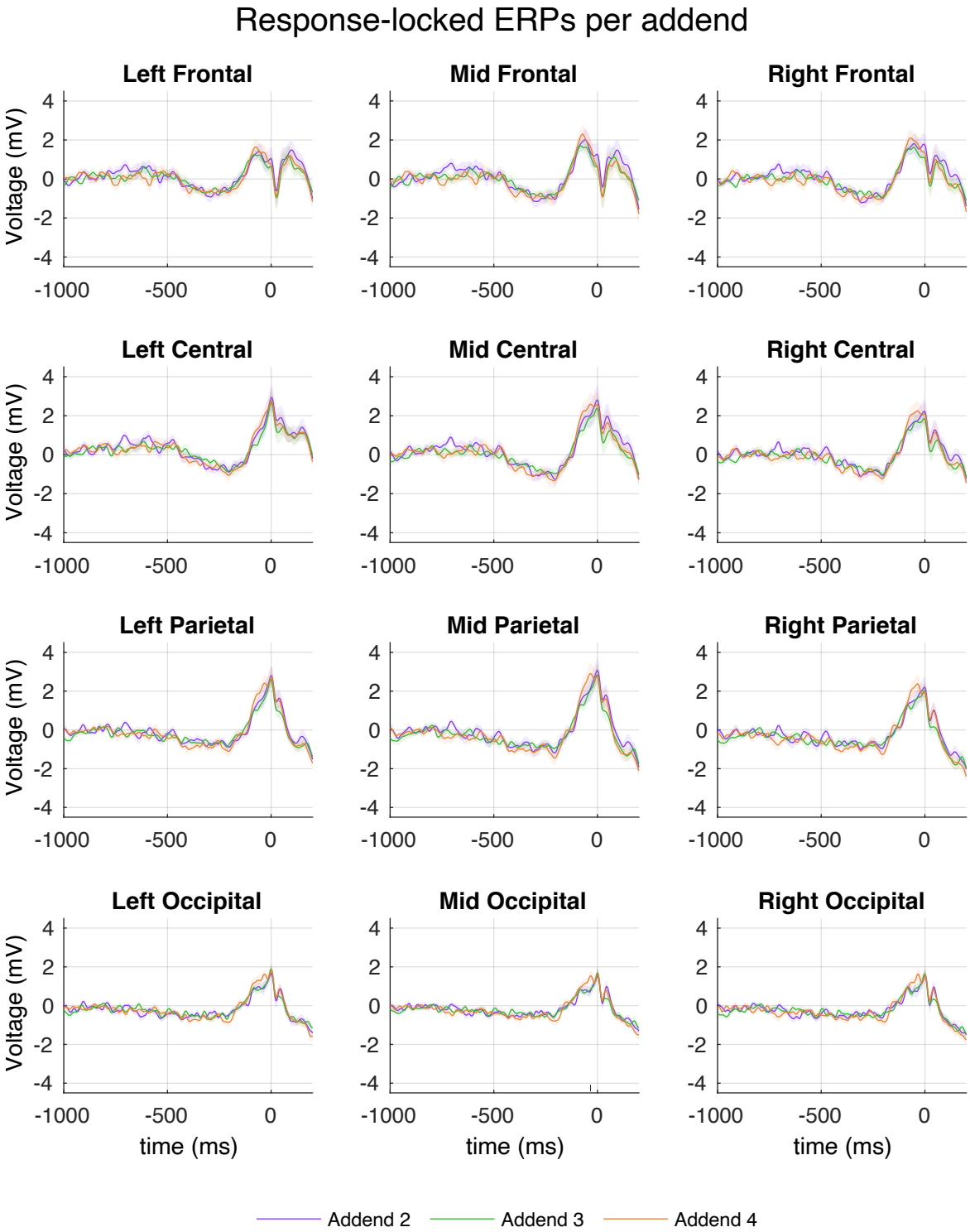

Figure A.1: Response-locked ERP waveforms from twelve regions for three addend conditions. Shaded areas indicate standard error of ERP signal of block associated by color. There are no temporal regions of Benjamini-Hochberg corrected significance.

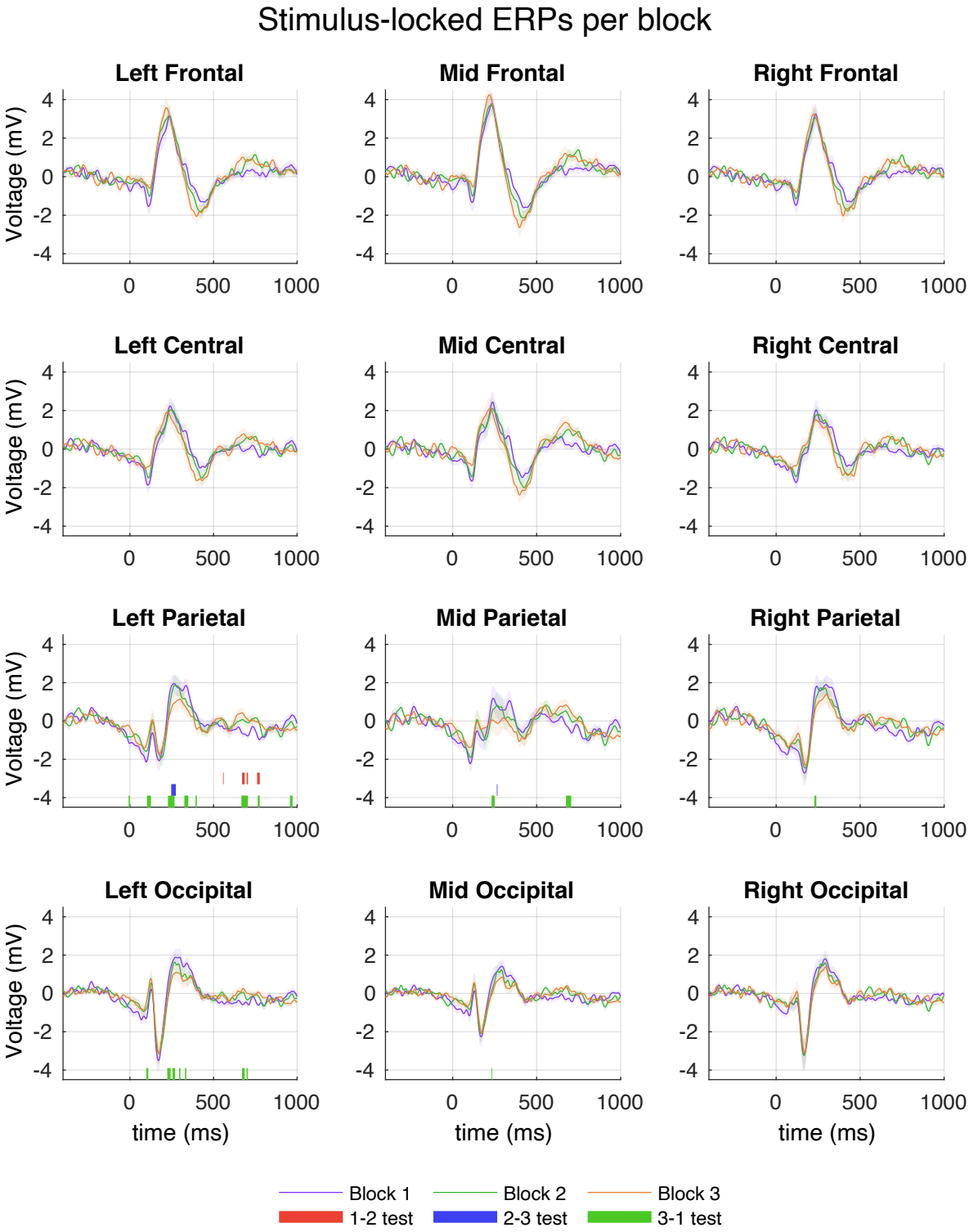

Figure A.2: Stimulus-locked ERP waveforms from twelve regions for three block conditions. Shaded areas indicate standard error of ERP signal of block associated by color. Bars at the bottom of the graphs indicate temporal regions of Benjamini-Hochberg corrected significance, pairwise as block 1-2, 2-3 and 3-1.

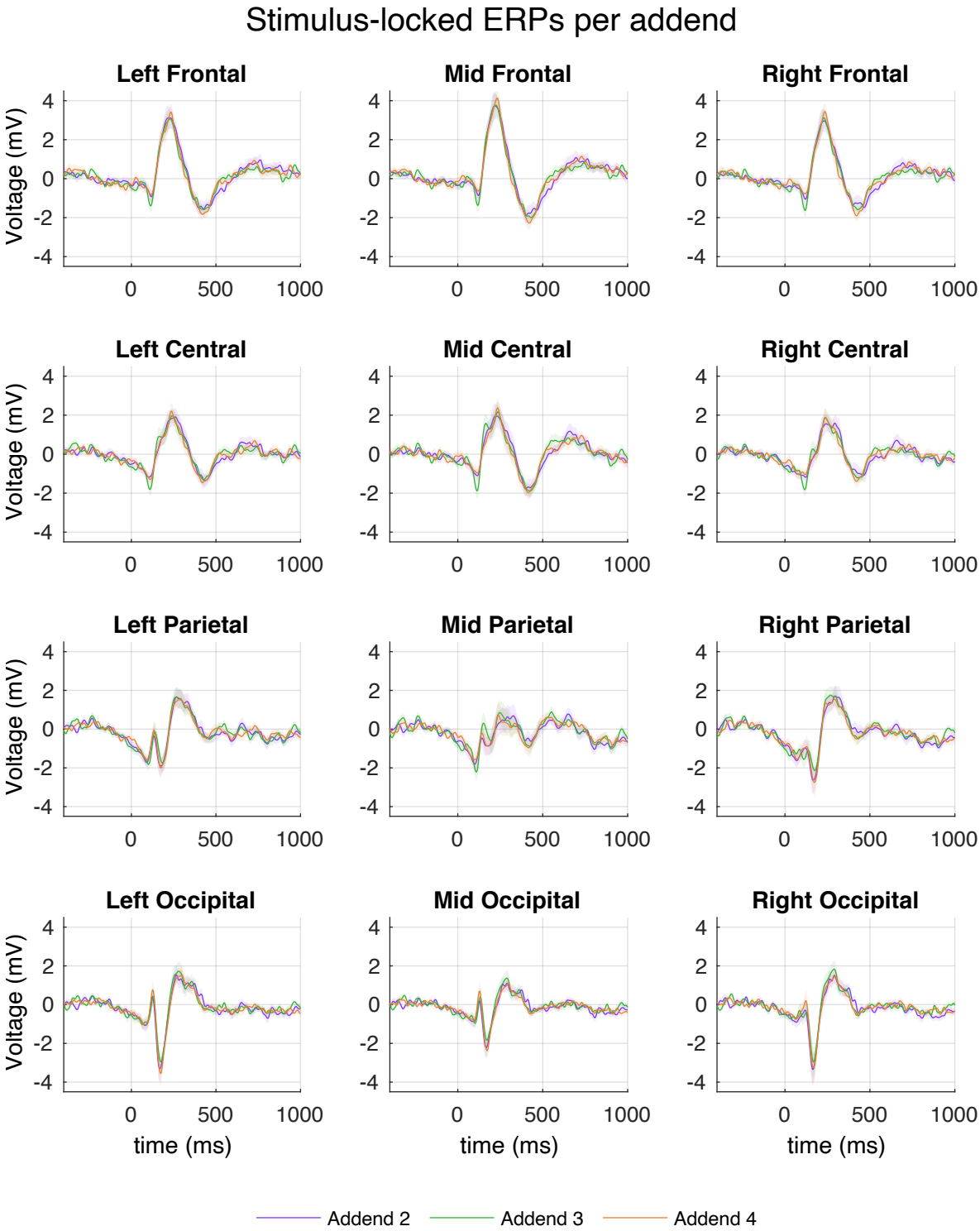

Figure A.3: Stimulus-locked ERP waveforms from twelve regions for three addend conditions. Shaded areas indicate standard error of ERP signal of block associated by color. There are no temporal regions of Benjamini-Hochberg corrected significance.